Organic & Biomolecular Chemistry

Cite this: *Org. Biomol. Chem.*, 2012, **10**, 5307

www.rsc.org/obc

PAPER

Isolation, antimicrobial activity, and absolute configuration of the furylidene tetronic acid core of pestalotic acids A–G†

Fan Zhang,‡[a] Gang Ding,‡[b] Li Li,[c] Xiaoyue Cai,[a] Yikang Si,[c] Liangdong Guo[a] and Yongsheng Che*[a,d]

Received 3rd March 2012, Accepted 16th May 2012
DOI: 10.1039/c2ob25469g

Natural products possessing the 3-(furan-2(5*H*)-ylidene)furan-2,4(3*H*,5*H*)-dione (furylidene tetronic acid) skeleton are rare and were encountered only as fungal metabolites. The configurational assignment of the furylidene tetronic acid core using conventional approaches remained a challenge. Pestalotic acids A–G (**1–7**) are new furylidene tetronic acid derivatives isolated from a plant endophyte *Pestalotiopsis yunnanensis*. The structure of **1** was elucidated by combination of NMR experiments, X-ray crystallography, and ECD calculations. Compounds **3** and **7** showed significant antimicrobial activity.

Introduction

Naturally occurring furylidene tetronic acids are a structurally unique and rarely encountered chemotype derived from a furylidene and a furan-2,4(3*H*,5*H*)-dione (tetronic acid) moiety *via* a carbon–carbon double bond. To date, the documented natural products of this class of were all produced by fungi. Examples include carlic and carolic acid,[1–3] terrestric acid,[3,4] dehydrocarolic acid,[3,5,6] italicic acid,[7] lowdenic acid (**9**),[8] and nodulisporacid A (**10**).[9] Due to the lack of appropriate functionality for chemical derivatization, and the isomerization of the furylidene double bond in all reported natural products, configurational assignment of the 4,4′-disubstituted furylidene tetronic acid core remained a challenge. The 4*R* absolute configuration for carolic acid and the 4*S* for carlic acid were individually assigned by X-ray analysis using Cu Kα radiation[2] and enantioselective synthesis,[3,10] whereas the 4*R*,4′*S* and 4*R*,4′*R*,6′*R* configurations were assigned by synthesis for terrestric acid[11] and nodulisporacid A,[12] respectively. Although electronic circular dichroism (ECD) characteristics of this class of natural products have not been reported and correlated with their absolute configurations, this approach would provide an alternative approach for configurational assignment of the 4,4′-disubstituted furylidene tetronic acid moiety.

This class of compounds attracted our attention when we first traced their presence in the EtOAc extract of an endolichenic *Pestalotiopsis* sp.[13] However, efforts to isolate enough material for structure elucidation was unsuccessful, either from this endolichenic strain or from other endophytic *Pestalotiopsis* spp. investigated.[14] Recently, we isolated two isoprenylated heterodimers with a new non-acyclic skeleton from a strain of *P. yunnanensis*,[15] but the isolated metabolites did not account for the antimicrobial activity of the crude extract. Therefore, the fungus was refermented in a larger scale to identify the active principles. Bioassay-guided fractionation of an EtOAc extract led to the isolation of seven new lowdenic acid analogues named pestalotic acids A–G (**1–7**), allowing us to assign the absolute configuration of the 4,4′-disubstituted furylidene tetronic acid moiety. Herein, we report the isolation, structure elucidation, and antimicrobial activity of these metabolites (Fig. 1).

Results and discussion

Pestalotic acid A (**1**) was assigned the molecular formula $C_{21}H_{30}O_6$ by HRESIMS (*m/z* 401.1938 $[M + Na]^+$; Δ −0.3 mmu). Its ^1H and ^{13}C NMR spectra showed resonances that were mostly duplicated in a ratio of approximately 1 : 1, suggesting the presence of an isomeric mixture. Although the two isomers were well-resolved on an HPLC column, analysis of each collected peak revealed both isomers, suggesting a spontaneous equilibration occurred. The chemical shifts for C-1 and C-3, and H-2′ and H-3′ for one isomer were obviously different from the other one, which were characteristic of an equilibrium mixture of the *E*- and *Z*-isomers.[7–9] Therefore, the structure elucidation was performed on the *Z*-isomer. Analysis of its NMR data (Table 1) revealed two methyl groups, 10 methylene units, one oxymethine (δ_H–δ_C 4.91 : 78.4), one oxygenated sp^3

[a]*State Key Laboratory of Mycology, Institute of Microbiology, Chinese Academy of Sciences, Beijing 100190, People's Republic of China. E-mail: cheys@im.ac.cn; Fax: +86 10 8261 8785*
[b]*Institute of Medicinal Plant Development, Chinese Academy of Medical Sciences and Peking Union Medical College, Beijing 100050, People's Republic of China*
[c]*Institute of Materia Medica, Chinese Academy of Medical Sciences and Peking Union Medical College, Beijing 100050, People's Republic of China*
[d]*Beijing Institute of Pharmacology & Toxicology, Beijing 100850, People's Republic of China*

†Electronic supplementary information (ESI) available: ^1H, ^{13}C NMR, CD spectra of **1–7**, and detailed computational data for **1**. CCDC 859983. For ESI and crystallographic data in CIF or other electronic format see DOI: 10.1039/c2ob25469g

‡These authors contributed equally to this work.

quaternary carbon (δ_C 102.0), four olefinic carbons (two of which are protonated), two carboxylic carbons (δ_C 167.5 and 173.0), and one α,β-unsaturated ketone carbon (δ_C 196.3). The ^1H–^1H COSY NMR data showed the isolated spin-systems of C-4–C-5, C-2′–C-3′, and C-5′–C-14′. Interpretation of the HMBC data established partial structures **a** and **b** (Fig. 2) with the C-5′–C-14′ aliphatic side chain attached to C-4′ in **b**. The relatively downfield shift for C-4′ (δ_C 102.0) and a coupling constant of 6.0 Hz between H-2′ and H-3′ implied that C-2′, C-3′, and C-4′ most likely located in a five-membered ring system.[16] HMBC correlations from H-2′ and H-3′ to C-1′ connected C-2′ to both C-1′ and C-3′. Although no HMBC cross-peaks were found to locate C-2, and to correlate C-1′ with substructure **a**, comparison of the NMR data of **1** with those of lowdenic acid[8] revealed the same furylidene tetronic acid moiety. Collectively, these data permitted a tentative assignment of the planar structure of **1**.

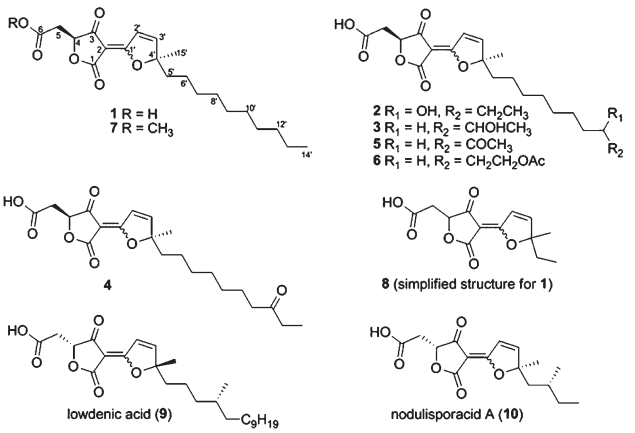

Fig. 1 Structures of pestalotic acids A–G (**1**–**7**), a simplified structure for pestalotic acid A (**8**), lowdenic acid (**9**), and nodulisporacid A (**10**).

The proposed structure of **1** was confirmed by X-ray crystallographic analysis on a crystal obtained from a solution of acetone–H_2O (10 : 1) freshly prepared in the dark. The X-ray data revealed the presence of only the *Z*-isomer in the crystal (Fig. 3), consistent with that observed for lowdenic acid.[8] The presence of traces of acid or the influence of light could break the equilibrium to favor the *Z*-isomer.[2,3,8,12]

The absolute configuration of **1** was deduced by comparison of the experimental and simulated ECD spectra generated by time-dependent density functional theory (TDDFT).[17] Since the aliphatic side chain is insignificant to the CD property of **1**, a

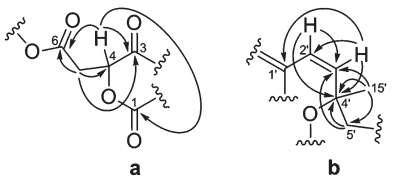

Fig. 2 Partial structures of **1** showing HMBC correlations.

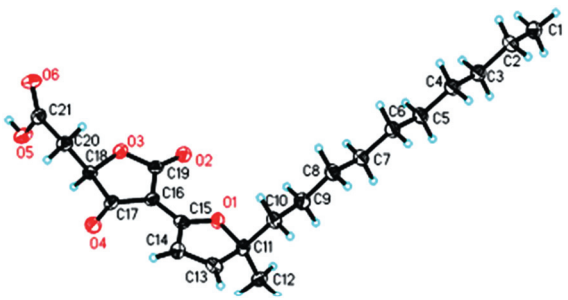

Fig. 3 Thermal ellipsoid representation of pestalotic acid A (**1**; *Z*-isomer). (Note: A different numbering system is used for the structural data deposited with the CCDC).

Table 1 NMR data of pestalotic acid A (**1**) in $CDCl_3$

Position	Pestalotic acid A (**1**)				
	δ_C[a]		δ_H[b] (mult., *J* in Hz)		HMBC
	E	*Z*	*E*	*Z*	
1	170.0, qC	167.5, qC			
2	93.6, qC	93.3, qC			
3	194.1, qC	196.3, qC			
4	78.1, CH	78.4, CH	4.87, dd (4.0, 7.5)	4.91, dd (4.0, 7.5)	1, 3, 6
5	35.8, CH_2	35.8, CH_2	3.05, dd (4.0, 17) 2.81, dd (7.5, 17)	3.02, dd (4.0, 17) 2.85, dd (7.5, 17)	3, 4, 6
6	173.0, qC	173.0, qC			
1′	179.4, qC	180.2, qC			
2′	123.3, CH	123.1, CH	7.50, d (6.0)	7.55, d (6.0)	1′, 3′, 4′
3′	160.3, CH	160.3, CH	7.43, d (6.0)	7.45, d (6.0)	1′, 2′, 4′
4′	102.5, qC	102.0, qC			
5′	38.1, CH_2	38.0, CH_2	1.92, m	1.98, m	3′, 4′, 6′, 7′
6′	24.0, CH_2	24.1, CH_2	1.20–1.33, m	1.20–1.33, m	
7′–11′	29.2–29.5, CH_2	29.2–29.5, CH_2	1.20–1.33, m	1.20–1.33, m	
12′	31.9, CH_2	31.9, CH_2	1.20–1.33, m	1.20–1.33, m	
13′	22.6, CH_2	22.6, CH_2	1.20–1.33, m	1.20–1.33, m	
14′	14.1, CH_3	14.1, CH_3	0.87, t (7.0)	0.87, t (7.0)	12′, 13′
15′	23.3, CH_3	23.2, CH_3	1.61, s	1.62, s	3′, 4′, 5′

[a] Recorded at 125 MHz. [b] Recorded at 500 MHz.

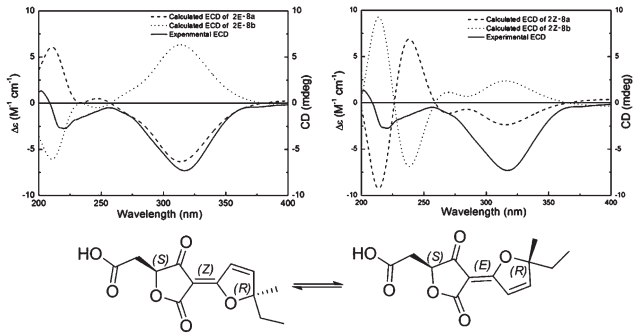

Fig. 4 Experimental CD spectrum of **1** in MeOH and calculated ECD spectra of the *E*- and *Z*-isomers of enantiomers **8a** and **8b** after a UV correction of 20 nm.

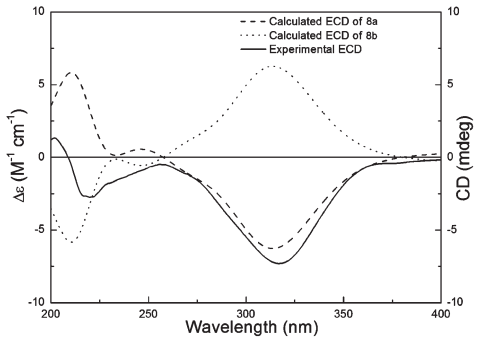

Fig. 5 Experimental CD spectrum of **1** in MeOH and calculated ECD spectra of the enantiomers (4*S*,4′*R*)-**8** (**8a**) and (4*R*,4′*S*)-**8** (**8b**) after a UV correction of 20 nm.

simplified structure **8** was used for ECD calculations. Considering the relative configuration secured for **1** by X-ray data, only the (4*S*,4′*R*)-**8** (**8a**) and (4*R*,4′*S*)-**8** (**8b**) configurations were calculated (Fig. 4). A systematic conformational analysis was performed for **8a** and **8b** *via* the Molecular Operating Environment (MOE) software package using the MMFF94 molecular mechanics force field calculation, which was further optimized using TDDFT at B3LYP/6-31G(d) basis set level in the gas phase within a 3 kcal mol^{-1} energy window, affording 12 and nine lowest-energy conformers for the *E*- and *Z*-isomers, respectively (Fig. S22 and S23†). The overall calculated ECD spectra of the two isomers were then generated by Boltzmann weighting of their lowest-energy conformers (Fig. 4). Conformation optimization and frequency calculation revealed the *E*-isomer was the major geometric isomer with a population of 76.6%, whereas the *Z*-isomer was located with a distribution of 23.4% (Fig. S22 and S23†). Therefore, the calculated ECD spectra of **8a** and **8b** were generated by Boltzmann weighting of their *E*- and *Z*-isomers corresponding to the above population. Since the ECD spectra were calculated in the gas phase, the solvent effect which could affect the proportions of the *E*- and *Z*-isomers was neglected. The absolute configuration of **1** was then extrapolated by comparison of the experimental calculated ECD spectra of **8a** and **8b** after a UV correction of 20 nm (Fig. S26†). The CD spectrum recorded for **1** matched the calculated ECD curve of **8a**, with negative Cotton effects (CEs) in the regions of 200–225 and 300–350 nm, but was opposite to that of **8b** (Fig. 5). Therefore, the 4*S*,4′*R* absolute configuration was deduced for **1**.

Pestalotic acid B (**2**) gave a pseudo molecular ion $[M + H]^+$ peak at *m/z* 395.2065 (Δ −0.1 mmu) by HRESIMS, consistent with the molecular formula $C_{21}H_{30}O_7$, which has one more oxygen atom than **1**. Its ^1H and ^{13}C NMR data (Table 2) revealed structural similarity to **1**, except that one methylene of the aliphatic chain was replaced by an oxymethine (δ_H–δ_C 3.43 : 72.6). The free hydroxy group was located at C-12′ on the basis of HMBC correlations from H_3-14′ to C-12′ and C-13′, completing the gross structure of **2**. The absolute configuration of C-4 and C-4′ in **2** was deduced by comparison of its CD data with those of **1**. The CD spectra of **1** and **2** (Fig. S15 and S16†) both showed negative CEs in 200–230 and 300–350 nm regions, suggesting the same 4*S*,4′*R* configuration for both compounds. However, attempts to assign the absolute configuration of C-12′ in **2** either by the modified Mosher's method,[18] or by obtaining a crystal suitable for X-ray crystallography were unsuccessful.

Pestalotic acid C (**3**) was assigned the same molecular formula $C_{21}H_{30}O_7$ as **2** on the basis of its HRESIMS data (*m/z* 395.2064 $[M + H]^+$; Δ +0.0 mmu). Its ^1H and ^{13}C NMR data (Table 2) revealed structural features nearly identical to those of **2**, except that the C-12′ oxymethine was shifted from 3.43 to 3.67 ppm, and the C-14′ methyl group was observed as a doublelet. These observations indicated that the free hydroxy group is located at C-13′ in **3**; this was supported by relevant ^1H–^1H COSY and HMBC correlations, allowing determination of the gross structure of **3**. The absolute configuration of C-4 and C-4′ in **3** was deduced by comparison of the CD spectrum of **3** with that of **1** (Fig. S15 and S17†), whereas the configuration of C-13′ could not be assigned due to the same reason as described above for **2**.

The elemental composition of pestalotic acid D (**4**) was established as $C_{21}H_{28}O_7$ by HRESIMS (*m/z* 393.1910 $[M + H]^+$; Δ −0.2 mmu). Comparison of the NMR data between **4** (Table 3) and **2** revealed the presence of one more ketone functionality (δ_C 213.6) and the absence of an oxymethine unit (δ_H–δ_C 3.43 : 72.6), indicating that the C-12′ methine carbon in **2** was oxidized to a ketone group in **4**; this was supported by HMBC correlations from H_2-11′, H_2-13′, and H_3-14′ to C-12′. The configuration of **4** was deduced as shown by analogy to **1**, and was supported by nearly identical CD spectra recorded for both compounds (Fig. S15 and S18†).

Pestalotic acid E (**5**) had the same molecular formula $C_{21}H_{28}O_7$ as **4** by HRESIMS (*m/z* 393.1909 $[M + H]^+$; Δ −0.1 mmu). Interpretation of its NMR data (Table 3) revealed the same core structure as **4**, except that H_3-14′ (δ_H 2.13) and H_2-12′ (δ_H 2.40) were observed as a singlet and a triplet, respectively, in the ^1H NMR spectrum of **5**, implying that C-13′ was a ketone carbon, which was supported by relevant HMBC correlations. The absolute configuration of **5** was also deduced by comparison of its CD spectrum with that of **1** (Fig. S15 and S19†).

The molecular formula of pestalotic acid F (**6**) was determined to be $C_{23}H_{32}O_8$ (HRESIMS; *m/z* 437.2172 $[M + H]^+$; Δ −0.2 mmu). The extra 58 mass units compared to **1**, suggested the presence of an acetyl group. Analysis of its NMR data (Table 4) revealed structural similarity to **1**, except that the C-14′ methyl (δ_H–δ_C 0.87 : 14.1) was replaced by an oxygenated

Table 2 NMR data of pestalotic acids B (**2**) and C (**3**) in acetone-d_6

	Pestalotic acid B (**2**)				Pestalotic acid C (**3**)			
Position	δ_C[a]		δ_H[b] (mult., *J* in Hz)		δ_C[a]		δ_H[b] (mult., *J* in Hz)	
	E	*Z*	*E*	*Z*	*E*	*Z*	*E*	*Z*
1	170.5, qC	167.6, qC			170.3, qC	167.3, qC		
2	94.3, qC	94.1, qC			94.1, qC	93.9, qC		
3	194.5, qC	197.2, qC			194.2, qC	197.0, qC		
4	79.3, CH	79.4, CH	4.81, dd (4.0, 6.5)	4.83, dd (4.0, 6.5)	79.1, CH	79.2, CH	4.81, dd (4.0, 6.5)	4.84, dd (4.0, 6.5)
5	36.3, CH_2	36.2, CH_2	2.94, dd (4.0, 17)	2.91, dd (4.0, 17)	36.1, CH_2	36.0, CH_2	2.95, dd (4.0, 18)	2.92, dd (4.0, 18)
			2.76, dd (6.5, 17)	2.80, dd (6.5, 17)			2.77, dd (8.0, 18)	2.80, dd (8.0, 18)
6	170.9, qC	170.9, qC			170.7, qC	170.7, qC		
1′	179.2, qC	180.1, qC			179.0, qC	179.9, qC		
2′	123.1, CH	123.1, CH	7.48, d (6.0)	7.38, d (6.0)	122.9, CH	122.9, CH	7.48, d (6.0)	7.38, d (6.0)
3′	162.0, CH	161.8, CH	7.83, d (6.0)	7.82, d (6.0)	161.7, CH	161.6, CH	7.83, d (6.0)	7.82, d (6.0)
4′	102.7, qC	102.2, qC			102.5, qC	102.0, qC		
5′	38.3, CH_2	38.2, CH_2	1.97, m	1.97, m	38.2, CH_2	38.1, CH_2	1.97, m	1.97, m
6′	24.5, CH_2	24.5, CH_2	1.27–1.45, m	1.27–1.45, m	24.3, CH_2	24.3, CH_2	1.26–1.39, m	1.26–1.39, m
7′–10′	26.4–30.0, CH_2	26.4–30.0, CH_2	1.27–1.45, m	1.27–1.45, m	26.3–30.0, CH_2	26.3–30.0, CH_2	1.26–1.39, m	1.26–1.39, m
11′	37.8, CH_2	37.7, CH_2	1.27–1.45, m	1.27–1.45, m	26.3–30.0, CH_2	26.3–30.0, CH_2	1.26–1.39, m	1.26–1.39, m
12′	72.6, CH	72.6, CH	3.43, m	3.43, m	40.0, CH_2	40.0, CH_2	1.26–1.39, m	1.26–1.39, m
13′	31.0, CH_2	31.0, CH_2	1.27–1.45, m	1.27–1.45, m	67.4, CH	67.3, CH	3.67, m	3.67, m
14′	10.3, CH_3	10.3, CH_3	0.88, t (7.5)	0.88, t (7.5)	23.8, CH_3	23.7, CH_3	1.09, d (6.5)	1.08, d (6.5)
15′	23.4, CH_3	23.3, CH_3	1.59, s	1.59, s	23.2, CH_3	23.2, CH_3	1.59, s	1.59, s

[a] Recorded at 100 MHz. [b] Recorded at 500 MHz.

Table 3 NMR data of pestalotic acids D (**4**) and E (**5**) in $CDCl_3$

	Pestalotic Acid D (**4**)				Pestalotic Acid E (**5**)			
Position	δ_C[a]		δ_H[b] (mult., *J* in Hz)		δ_C[a]		δ_H[b] (mult., *J* in Hz)	
	E	*Z*	*E*	*Z*	*E*	*Z*	*E*	*Z*
1	170.0, qC	167.7, qC			170.2, qC	167.8, qC		
2	93.8, qC	93.6, qC			93.7, qC	93.7, qC		
3	194.2, qC	196.6, qC			194.3, qC	196.6, qC		
4	78.2, CH	78.4, CH	4.81, dd (4.0, 7.0)	4.88, dd (4.0, 7.0)	78.4, CH	78.6, CH	4.86, dd (4.0, 6.4)	4.89, dd (4.0, 6.4)
5	35.8, CH_2	35.9, CH_2	3.06, dd (4.0, 17)	3.02, dd (4.0, 17)	36.0, CH_2	36.0, CH_2	3.04, dd (4.0, 17)	3.00, dd (4.0, 17)
			2.84, dd (7.0, 17)	2.97, dd (7.0, 17)			2.82, dd (6.4, 17)	2.86, dd (6.4, 17)
6	172.0, qC	172.0, qC			173.6, qC	173.6, qC		
1′	179.3, qC	179.8, qC			179.3, qC	180.0, qC		
2′	123.0, CH	123.0, CH	7.50, d (6.0)	7.57, d (6.0)	123.3, CH	123.3, CH	7.48, d (6.0)	7.54, d (6.0)
3′	160.0, CH	160.2, CH	7.43, d (6.0)	7.45, d (6.0)	160.1, CH	160.3, CH	7.42, d (6.0)	7.44, d (6.0)
4′	102.4, qC	101.6, qC			102.4, qC	101.7, qC		
5′	38.0, CH_2	37.8, CH_2	1.90, m	2.01, m	38.0, CH_2	37.8, CH_2	1.90, m	1.99, m
6′	23.8, CH_2	23.8, CH_2	1.11–1.25, m	1.11–1.25, m	23.9, CH_2	23.9, CH_2	1.12–1.30, m	1.12–1.30, m
7′–9′	28.7–29.2, CH_2	28.7–29.2, CH_2	1.11–1.25, m	1.11–1.25, m	29.0–29.3, CH_2	29.0–29.3, CH_2	1.12–1.30, m	1.12–1.30, m
10′	23.3, CH_2	23.3, CH_2	1.53, m	1.53, m	29.0–29.3, CH_2	29.0–29.3, CH_2	1.12–1.30, m	1.12–1.30, m
11′	42.2, CH_2	42.2, CH_2	2.40, m	2.40, m	23.6, CH_2	23.6, CH_2	1.53, m	1.53, m
12′	211.9, qC	213.6, qC			43.7, CH_2	43.7, CH_2	2.40, t (7.2)	2.40, t (7.2)
13′	35.9, CH_2	35.9, CH_2	2.40, m	2.40, m	209.5, qC	210.3, qC		
14′	7.8, CH_3	7.8, CH_3	1.04, t (7.0)	1.04, t (7.0)	29.9, CH_3	29.9, CH_3	2.13, s	2.13, s
15′	23.5, CH_3	23.5, CH_3	1.62, s	1.62, s	23.3, CH_3	23.3, CH_3	1.60, s	1.60, s

[a] Recorded at 100 MHz. [b] Recorded at 400 MHz.

methylene (δ_H–δ_C 3.96 : 63.7). In addition, NMR resonances for an acetyl group (δ_H–δ_C 1.98 : 20.7, 170.4) were observed, indicating that the C-14′ oxygen is acylated in **6**, which was supported by HMBC correlations from H_2-14′ and H_3-17′ to C-16′. The absolute configuration of **6** was deduced as shown by comparing the CD spectrum of **6** with **1** (Fig. S15 and S20†).

Pestalotic acid G (**7**) was assigned the molecular formula $C_{22}H_{32}O_6$ (HRESIMS; *m/z* 393.2271 $[M + H]^+$; Δ +0.1 mmu), 14 mass units more than that of **1**. Comparison of the NMR data between **7** (Table 4) and **1** revealed that the carboxylic acid group in **1** was methylated in **7**, as supported by an HMBC correlation from H_3-7 to C-6. Therefore, the gross structure of

Table 4 NMR data of pestalotic acids F (**6**) and G (**7**)

Position	Pestalotic acid F (**6**)				Pestalotic acid G (**7**)			
	δ_C[a]		δ_H[b] (mult., *J* in Hz)		δ_C[c]		δ_H[d] (mult., *J* in Hz)	
	E	*Z*	*E*	*Z*	*E*	*Z*	*E*	*Z*
1	169.8, qC	167.1, qC			170.2, qC	167.6, qC		
2	93.2, qC	93.0, qC			93.8, qC	93.5, qC		
3	194.0, qC	196.4, qC			194.3, qC	196.4, qC		
4	78.4, CH	78.6, CH	4.80, dd (4.0, 6.4)	4.84, dd (4.0, 6.4)	78.5, CH	78.7, CH	4.88, dd (4.0, 7.0)	4.90, dd (4.0, 7.0)
5	35.8, CH_2	35.8, CH_2	2.94, dd (4.0, 17) 2.66, dd (6.4, 17)	2.91, dd (4.0, 17) 2.70, dd (6.4, 17)	36.0, CH_2	36.1, CH_2	3.02, dd (4.0, 18) 2.80, dd (7.0, 18)	2.98, dd (4.0, 18) 2.83, dd (7.0, 18)
6	170.7, qC	170.7, qC			169.7, qC	169.7, qC		
7					52.2, CH_3	52.2, CH_3	3.71, s	3.71, s
1′	178.0, qC	178.9, qC			179.1, qC	179.9, qC		
2′	121.6, CH	121.6, CH	7.27, d (6.0)	7.37, d (6.0)	123.3, CH	123.1, CH	7.50, d (6.0)	7.56, d (6.0)
3′	162.5, CH	162.4, CH	7.94, d (6.0)	7.94, d (6.0)	159.9, CH	160.0, CH	7.42, d (6.0)	7.43, d (6.0)
4′	102.1, qC	101.5, qC			102.3, qC	101.8, qC		
5′	36.9, CH_2	36.9, CH_2	1.89, m	1.89, m	38.1, CH_2	38.0, CH_2	1.91, m	2.00, m
6′	23.2–28.8, CH_2	24.5, CH_2	1.05–1.30, m	1.05–1.30, m	24.0, CH_2	24.1, CH_2	1.18–1.32, m	1.18–1.32, m
7′–11′	23.2–28.8, CH_2	26.4–30.0, CH_2	1.05–1.30, m	1.05–1.30, m	29.3–29.5, CH_2	29.3–29.5, CH_2	1.18–1.32, m	1.18–1.32, m
12′	25.3, CH_2	25.3, CH_2	1.05–1.30, m	1.05–1.30, m	31.9, CH_2	31.9, CH_2	1.18–1.32, m	1.18–1.32, m
13′	28.2, CH_2	28.2, CH_2	1.52, m	1.52, m	22.7, CH_2	22.7, CH_2	1.18–1.32, m	1.18–1.32, m
14′	63.7, CH_2	63.7, CH_2	3.96, t (6.4)	3.96, t (6.4)	14.1, CH_3	14.1, CH_3	0.88, d (6.5)	0.88, d (6.5)
15′	22.7, CH_3	22.7, CH_3	1.51, s	1.52, s	23.4, CH_3	23.3, CH_3	1.62, s	1.62, s
16′	170.4, qC	170.4, qC						
17′	20.7, CH_3	20.7, CH_3	1.98, s	1.98, s				

[a] Recorded at 100 MHz in DMSO-d_6. [b] Recorded at 400 MHz in DMSO-d_6. [c] Recorded at 125 MHz in $CDCl_3$. [d] Recorded at 500 MHz in $CDCl_3$.

Table 5 Antibacterial activity of compounds **3**, **6**, and **7**

Compound	IC_{50}/MIC (μM)	
	S. aureus	*S. pneumoniae*
3	1.83 ± 0.208/6.35	4.44 ± 0.20/12.69
6	42.98 ± 0.48/>45.87	39.08 ± 0.55/>45.87
7	4.85 ± 0.01/6.38	2.98 ± 0.15/12.76
Ampicillin	0.06 ± 0.009/0.46	1.09 ± 0.09/28.65

7 was established with its configuration similarly deduced by analogy to **1** (Fig. S15 and S21†).

Compounds **1–7** were tested for antibacterial activity against the Gram-positive bacteria, *Staphylococcus aureus* Col (CGMCC 1.2465) and *Streptococcus pneumoniae* (CGMCC 1.1692) (Table 5). Compounds **3** and **7** showed significant activity against the pathogens, with MIC values of 6.35–12.76 μM (Table 5), while the positive control ampicillin showed MIC values of 0.46 and 28.65 μM, respectively.

Pestalotic acids A–G (**1–7**) are closely related to lowdenic acid,[8] but differ by having different aliphatic chains. Due to the lack of any useful NOESY correlations and the difficulty in obtaining crystals suitable for X-ray crystallographic analysis using Cu Kα radiation, configurational assignment has relied on synthesis prior to this report. For example, nodulisporacid A (**10**), an analogue of lowdentic acid and the pestalotic acids, was assigned the 4*R*,4′*R*,6′*R* configuration by synthesis. Specifically, methyl esters for four of the eight possible isomers of **10**, (4*S*,4′*S*,6′*S*), (4*S*,4′*R*,6′*S*), (4*R*,4′*S*,6′*S*), and (4*R*,4′*R*,6′*S*) were prepared and compared with the natural product.[12] Only the ^{1}H NMR data of the (4*S*,4′*S*,6′*S*)-isomer were consistent with the authentic sample, whereas those of other three isomers showed slightly different chemical shifts for the asterisked carbons. In addition, the specific rotation of the synthetic (4*S*,4′*S*,6′*S*)-isomer ($[\alpha]_D^{28}$ −0.96) was much smaller than the natural product ($[\alpha]_D^{27}$ −20.6).[9] The ^{1}H NMR data of the (*R*)-1-phenylethyamine derivative for the (4*S*,4′*S*,6′*S*)-isomer of **10** matched well with those of the (*S*)-1-phenylethyamine derivative. Therefore, the authors proposed the 4*R*,4′*R*,6′*R* configuration for nodulisporacid A.[12] However, the (4*R*,4′*R*,6′*R*)-isomer was not synthesized to support this conclusion.

Conclusions

In the current work, the absolute configuration of **1** was deduced by a combination of X-ray crystallography and ECD calculations, representing the first configurational assignment of the 4,4′-disubstituted furylidene tetronic acid moiety using such an approach. Based on our results, lowdenic acid is likely to have the same absolute configuration as **1–7**. The discovery of **1–7** further expanded the structural diversity of this rare class of natural products and provided an alternative way for their configurational assignment.

Experimental section

General experimental procedures

Optical rotations were measured on a Perkin-Elmer 241 polarimeter, and UV data were obtained on a Shimadzu Biospec-1601 spectrophotometer. CD spectra were recorded on a JASCO J-815 spectropolarimeter. IR data were obtained using a Nicolet

Magna-IR 750 spectrophotometer. ^{1}H and ^{13}C NMR data were acquired with Varian Mercury-400 and Inova-500 spectrometers using solvent signals ($CDCl_3$: δ_H 7.26/δ_C 77.6; acetone-d_6: δ_H 2.05/δ_C 29.8, 206.1; DMSO-d_6: δ_H 2.50/δ_C 39.5) as references. The HMQC and HMBC experiments were optimized for 145.0 and 8.0 Hz, respectively. HRESIMS data were obtained using an Agilent Accurate-Mass-Q-TOF LC/MS 6520 instrument equipped with an electrospray ionization (ESI) source. The fragmentor and capillary voltages were kept at 125 and 3500 V, respectively. Nitrogen was supplied as the nebulizing and drying gas. The temperature of the drying gas was set at 300 °C. The flow rate of the drying gas and the pressure of the nebulizer were 10 L min^{-1} and 10 psi, respectively. All MS experiments were performed in positive ion mode. Full-scan spectra were acquired over a scan range of *m*/*z* 100–1000 at 1.03 spectra/s.

Fungal material and fermentation

The culture of *P. yunnanensis* was isolated from the branches of *Podocarpus macrophyllus* (Thunb.) D. Don at Kunming World Horticultural Exposition Garden, Kunming, People's Republic of China, in November, 2002. The isolate was identified by one of the authors (L.G.) based on morphology and sequence (Genbank Accession No. AY373375) analysis of the ITS region of the rDNA and assigned the accession number 789 in L.G.'s culture collection at the Institute of Microbiology, Chinese Academy of Sciences, Beijing. The strain was cultured on slants of potato dextrose agar (PDA) at 25 °C for 10 days. Agar plugs were cut into small pieces (about 0.5 × 0.5 × 0.5 cm^3) under aseptic conditions, 15 of these pieces were used to inoculate in three Erlenmeyer flasks (250 mL), each containing 50 mL of media (0.4% glucose, 1% malt extract, and 0.4% yeast extract); the final pH of the media was adjusted to 6.5 and sterilized by autoclave. Three flasks of the inoculated media were incubated at 25 °C on a rotary shaker at 170 rpm for five days to prepare the seed culture. Spore inoculum was prepared by suspension in sterile, distilled H_2O to give a final spore/cell suspension of 1 × 10^6 mL^{-1}. Fermentation was carried out in eight Fernbach flasks (500 mL), each containing 80 g of rice. Distilled H_2O (120 mL) was added to each flask, and the contents were soaked overnight before autoclaving at 15 psi for 30 min. After cooling to room temperature, each flask was inoculated with 5.0 mL of the spore inoculum and incubated at 25 °C for 40 days.

Extraction and isolation

The fermented material was extracted with EtOAc (3 × 500 mL), and the organic solvent was evaporated to dryness under vacuum to afford the crude extract (15 g), which was fractionated by silica gel VLC using petroleum ether–EtOAc gradient elution. The fraction (356 mg) eluted with 30% EtOAc was separated by Sephadex LH-20 column chromatography (CC) eluting with 1 : 1 CH_2Cl_2–MeOH, and the resulting subfractions were further purified by semipreparative RP HPLC (Agilent Zorbax SB-C_{18} column; 5 μm; 9.4 × 250 mm; 78% MeCN in H_2O for 25 min; 2 mL min^{-1}) to afford **7** (2.5 mg, t_R 18.0 min). Fractions (650 mg) eluted with 40–50% EtOAc were separated by Sephadex LH-20 CC eluting with MeOH, and the resulting subfractions were purified by RP HPLC (55% MeCN in H_2O for 2 min, followed by 55–75% over 30 min; 2 mL min^{-1}) to afford **1** (50 mg, t_R 19.9 min). The fraction (450 mg) eluted with 60% EtOAc was separated by Sephadex LH-20 CC (MeOH) and RP HPLC to afford **4** (4.0 mg, t_R 29.5 min; 38% MeCN in H_2O for 30 min; 2 mL min^{-1}), **5** (45 mg, t_R 26.5 min), and **6** (8.0 mg, t_R 34.0 min; 47% MeCN in H_2O for 35 min; 2 mL min^{-1}). Fractions (550 mg) eluted with 70–100% EtOAc were separated by Sephadex LH-20 CC (MeOH) and RP HPLC (35% MeCN in H_2O for 40 min; 2 mL min^{-1}) to afford **2** (5.0 mg, t_R 34.5 min) and **3** (15 mg, t_R 28.3 min).

Pestalotic acid A (1). Colorless needles (acetone–H_2O 10 : 1); mp 94–96 °C; $[\alpha]_D^{25}$ −159 (*c* 0.40, MeOH); UV (MeOH) λ_{max}/nm (logε) 213 (4.13), 313 (4.40); IR (neat) ν_{max} 3116, 2918, 2852, 1757, 1734, 1710, 1599, 1573, 1178, 1153, 999 cm^{-1}; ^{1}H, ^{13}C NMR, and HMBC data see Table 1; HRESIMS *m*/*z* 401.1938 (calcd for $C_{21}H_{30}O_6Na$, 401.1935).

Pestalotic acid B (2). Colorless oil; $[\alpha]_D^{25}$ −197 (*c* 0.21, MeOH); UV (MeOH) λ_{max}/nm (log ε) 212 (4.16), 313 (4.43); IR (neat) ν_{max} 3452, 3079, 2932, 2857, 1754, 1735, 1701, 1591, 1567, 1357, 1175, 1049, 1022, 995 cm^{-1}; H and ^{13}C NMR data see Table 2; HMBC data (400 MHz; acetone-d_6) H-4 → C-1, 3, 5, 6; H_2-5 → C-3, 4, 6; H-2′ → C-1′, 3′, 4′; H-3′ → C-1′, 2′, 4′; H_2-5′ → C-3′, 4′, 6′, 7′; H-12′ → C-10′; H_3-14′ → C-12′, 13′; H_3-15′ → C-3′, 4′, 5′; HRESIMS *m*/*z* 395.2065 (calcd for $C_{21}H_{31}O_7$, 395.2064).

Pestalotic acid C (3). White powder; $[\alpha]_D^{25}$ −174 (*c* 0.10, MeOH); UV (MeOH) λ_{max}/nm (log ε) 213 (4.11), 313 (4.40); IR (neat) ν_{max} 3527, 3081, 2966, 2924, 2852, 1754, 1699, 1588, 1566, 1181, 1048, 1023, 1001 cm^{-1}; H and ^{13}C NMR data see Table 2; HMBC data (400 MHz; acetone-d_6) H-4 → C-1, 3, 5, 6; H_2-5 → C-3, 4, 6; H-2′ → C-1′, 3′, 4′; H-3′ → C-1′, 2′, 4′; H_2-5′ → C-3′, 4′, 6′, 7′; H-13′ → C-14′; H_3-14′ → C-12′, 13′; H_3-15′ → C-3′, 4′, 5′; HRESIMS *m*/*z* 395.2064 (calcd for $C_{21}H_{31}O_7$, 395.2064).

Pestalotic acid D (4). White powder; $[\alpha]_D^{25}$ −169 (*c* 0.12, MeOH); UV (MeOH) λ_{max}/nm (log ε) 217 (3.82), 321 (4.14); IR (neat) ν_{max} 3080, 2934, 2858, 1755, 1703, 1592, 1567, 1160, 1048, 1021, 993 cm^{-1}; H and ^{13}C NMR data see Table 3; HMBC data (400 MHz; $CDCl_3$) H-4 → C-3, 5, 6; H_2-5 → C-3, 4, 6; H-2′ → C-1′, 3′, 4′; H-3′ → C-1′, 2′, 4′; H_2-5′ → C-3′, 4′, 6′, 7′; H_2-10′ → C-9′, 11′; H_2-11′ → C-10′, 12′; H_2-13′ → C-12′, 14′; H_3-14′ → C-12′, 13′; H_3-15′ → C-3′, 4′, 5′; HRESIMS *m*/*z* 393.1910 (calcd for $C_{21}H_{29}O_7$, 393.1908).

Pestalotic acid E (5). White powder; $[\alpha]_D^{25}$ −193 (*c* 0.10, MeOH); UV (MeOH) λ_{max}/nm (log ε) 217 (4.22), 322 (4.52); IR (neat) ν_{max} 3080, 2932, 2857, 1755, 1703, 1590, 1567, 1357, 1169, 1048, 1021, 993 cm^{-1}; H and ^{13}C NMR data see Table 3; HMBC data (400 MHz; $CDCl_3$) H-4 → C-6; H_2-5 → C-4, 6; H-2′ → C-1′, 3′, 4′; H-3′ → C-1′, 2′, 4′; H_2-5′ → C-3′, 4′, 6′, 7′; H_2-11′ → C-10′, 12′, 13′; H_2-12′ → C-11′, 13′, 14′; H_3-14′ → C-12′, 13′; H_3-15′ → C-3′, 4′, 5′; HRESIMS *m*/*z* 393.1909 (calcd for $C_{21}H_{29}O_7$, 393.1908).

Pestalotic acid F (6). White powder; $[\alpha]_D^{25}$ −143 (*c* 0.10, MeOH); UV (MeOH) λ_{max}/nm (log ε) 218 (4.07), 322 (4.41);

IR (neat) ν_{max} 3117, 2920, 2854, 1756, 1736, 1709, 1599, 1575, 1243, 1179, 1155, 1050, 1000 cm^{-1}; H and ^{13}C NMR data see Table 4; HMBC data (400 MHz; DMSO-d_6) H-4 → C-3, 5, 6; H_2-5 → C-3, 4, 6; H-2′ → C-1′, 3′, 4′; H-3′ → C-1′, 2′, 4′; H_2-5′ → C-3′, 4′, 15′; H_2-13′ → C-12′, 14′; H_2-14′ → C-12′, 13′, 16′; H_3-15′ → C-3′, 4′, 5′; H_3-17′ → C-16′; HRESIMS *m*/*z* 437.2172 (calcd for $C_{23}H_{33}O_8$, 437.2170).

Pestalotic acid G (7). Colorless oil; $[\alpha]_D^{25}$ −153 (*c* 0.20, MeOH); UV (MeOH) λ_{max}/nm (log ε) 218 (4.04), 323 (4.31); IR (neat) ν_{max} 3080, 2927, 2855, 1745, 1704, 1594, 1568, 1168, 1049, 1022, 989 cm^{-1}; H and ^{13}C NMR data see Table 4; HMBC data (500 MHz; $CDCl_3$) H-4 → C-3, 5, 6; H_2-5 → C-3, 4, 6; H_3-7 → C-6; H-2′ → C-1′, 3′, 4′; H-3′ → C-1′, 2′, 4′; H_2-5′ → C-3′, 4′, 6′, 7′; H_3-14′ → C-12′, 13′; H_3-15′ → C-3′, 4′, 5′; HRESIMS *m*/*z* 393.2271 (calcd for $C_{22}H_{32}O_6$, 393.2272).

X-ray crystallographic analysis of pestalotic acid A (1)[19]

Upon crystallization from acetone–H_2O (10 : 1) using the vapor diffusion method, colorless crystals were obtained for **1**. A crystal (0.34 × 0.28 × 0.06 mm) was separated from the sample and mounted on a glass fiber, and data were collected using a Bruker SMART 1000 CCD diffractometer with graphite-monochromated Mo Kα radiation, λ = 0.71073 Å at 173 (2) K. Crystal data: $C_{42}H_{62}O_{13}$, $2M + H_2O$ = 774.92, space group Monoclinic, C2; unit cell dimensions a = 56.216(11) Å, b = 4.9368(10) Å, c = 15.390(3) Å, V = 4186.6(15) $Å^3$, Z = 4, D_{calcd} = 1.229 mg m^{-3}, μ = 0.090 mm^{-1}, $F(000)$ = 1672. The structure was solved by direct methods using SHELXL-97[20] and refined using full-matrix least-squares difference Fourier techniques. All non-hydrogen atoms were refined with anisotropic displacement parameters, and all hydrogen atoms were placed in idealized positions and refined as riding atoms with the relative isotropic parameters. Absorption corrections were applied with the Siemens Area Detector Absorption Program (SADABS).[21] The 20 380 measurements yielded 7681 independent reflections after equivalent data were averaged, and Lorentz and polarization corrections were applied. The final refinement gave R_1 = 0.0853 and wR_2 = 0.1754 [$I > 2\sigma(I)$].

Computational details

Systematic conformational analyses for **8a** and **8b** were performed *via* the Molecular Operating Environment (MOE) ver. 2009.10. (Chemical Computing Group, Canada) software package using the MMFF94 molecular mechanics force field calculation, which were further optimized using TDDFT at B3LYP/6-31G(d) basis set level in the gas phase. The stationary points have been checked as the true minima of the potential energy surface by verifying they do not exhibit vibrational imaginary frequencies. The 20 lowest electronic transitions were calculated and the rotational strengths of each electronic excitation were given using both dipole length and dipole velocity representations. ECD spectra were stimulated using a Gaussian function with a half-bandwidth of 0.4 eV. Equilibrium populations of conformers at 298.15 K were calculated from their relative free energies (ΔG) using Boltzmann statistics. The overall ECD spectra were then generated according to Boltzmann weighting of each conformer. The systematic errors in the prediction of the wavelength and excited-state energies are compensated for by employing UV correlation. All quantum computations were performed using Gaussian03 package,[22] on an IBM cluster machine located at the High Performance Computing Center of Peking Union Medical College.

Antibacterial assay[23]

The antibacterial assay was conducted in triplicate following the National Center for Clinical Laboratory Standards (NCCLS) recommendations.[24] The strains *Staphylococcus aureus* Col (CGMCC 1.2465) and *Streptococcu pneumoniae* (CGMCC 1.1692) were grown on Mueller-Hinton broth (MHB). Targeted microbes (3–4 colonies) were cultured in broth culture (37 °C for 24 h), and the final suspension of bacteria in MHB medium was 10^6 cells per mL. Test samples (10 mg mL^{-1} as stock solution in DMSO and serial dilutions) were transferred to a 96-well clear plate in triplicate, and the suspension of the test organisms was added to each well, achieving a final volume of 200 µL (ampicillin was used as the positive control). After incubation at 37 °C for 24 h, the absorbance at 595 nm was measured with a microplate reader (TECAN). The inhibition was calculated and plotted *versus* test concentrations to afford the IC_{50}, whereas the MIC was defined as the lowest concentration that completely inhibited the growth of the test organism.[25]

Acknowledgements

We gratefully acknowledge financial support from the National Natural Science Foundation of China (30925039), the Beijing Natural Science Foundation (5111003), the Ministry of Science and Technology of China (2010ZX09401-403 and 2012ZX09301-003), and the Chinese Academy of Sciences (KSCX2-EW-G-6).

Notes and references

1 P. W. Clutterbuck, W. N. Haworth, H. Raistrick, G. Smith and M. Stacey, *Biochem. J.*, 1934, **28**, 94–110.
2 O. Simonsen, T. Reffstrup and P. M. Boll, *Tetrahedron*, 1980, **36**, 795–797.
3 J. P. Jacobsen, T. Reffstrup, R. E. Cox, J. S. E. Holker and P. M. Boll, *Tetrahedron Lett.*, 1978, **12**, 1081–1084.
4 J. H. Birkinshaw and H. Raistrick, *Biochem. J.*, 1936, **30**, 2194–2200.
5 A. Bracken and H. Raistrick, *Biochem. J.*, 1947, **41**, 569–575.
6 K. A. Alvi, B. G. Nair, J. Rabenstein, G. Davis and D. D. Baker, *J. Antibiot.*, 2000, **53**, 110–113.
7 K. Arai, H. Miyajima, T. Mushiroda and Y. Yamamoto, *Chem. Pharm. Bull.*, 1989, **37**, 3229–3235.
8 R. F. Angawi, D. C. Swenson, J. B. Gloer and D. T. Wicklow, *J. Nat. Prod.*, 2003, **66**, 1259–1262.
9 C. Kasettrathat, N. Ngamrojanavanich, S. Wiyakrutta, C. Mahidol, S. Ruchirawat and P. Kittakoop, *Phytochemistry*, 2008, **69**, 2621–2626.
10 P. M. Booth, C. M. J. Fox and S. V. Ley, *J. Chem. Soc., Perkin Trans. 1*, 1987, 121–129.
11 P. M. Boll, E. Sørensen and E. Balieu, *Acta Chem., Scand.*, 1968, **22**, 3251–3255.
12 T. Sumiya, K. Ishigami and H. Watanabe, *Tetrahedron Lett.*, 2010, **51**, 2765–2767.
13 G. Ding, Y. Li, S. Fu, S. Liu, J. Wei and Y. Che, *J. Nat. Prod.*, 2009, **72**, 182–186.
14 (*a*) G. Ding, Z. Zheng, S. Liu, H. Zhang, L. Guo and Y. Che, *J. Nat. Prod.*, 2009, **72**, 942–945; (*b*) L. Liu, S. Liu, X. Chen, L. Guo and

Y. Che, *Bioorg. Med. Chem.*, 2009, **17**, 606–613; (*c*) L. Liu, Y. Li, S. Liu, Z. Zheng, X. Chen, H. Zhang, L. Guo and Y. Che, *Org. Lett.*, 2009, **11**, 2836–2839; (*d*) L. Liu, S. Niu, X. Lu, X. Chen, H. Zhang, L. Guo and Y. Che, *Chem. Commun.*, 2010, **46**, 460–462; (*e*) L. Liu, T. Bruhn, L. Guo, D. C. G. Götz, R. Brun, A. Stich, Y. Che and G. Bringmann, *Chem.–Eur. J.*, 2011, **17**, 2604–2613.

15 G. Ding, F. Zhang, H. Chen, L. Guo, Z. Zou and Y. Che, *J. Nat. Prod.*, 2011, **74**, 286–291.

16 E. Pretsch, J. Seibl, W. Simon and T. Clerc, *Tables of Spectral Data for Structure Determination of Organic Compounds*, Springer-Verlag, Berlin, 1981, p. H230.

17 (*a*) C. Diedrich and S. Grimme, *J. Phys. Chem. A*, 2003, **107**, 2524–2539; (*b*) T. D. Crawford, M. C. Tam and M. L. Abrams, *J. Phys. Chem. A*, 2007, **111**, 12057–12068; (*c*) P. J. Stephens, F. J. Devlin, F. Gasparrini, A. Ciogli, D. Spinelli and B. Cosimelli, *J. Org. Chem.*, 2007, **72**, 4707–4715; (*d*) Y. Ding, X. C. Li and D. Ferreira, *J. Org. Chem.*, 2007, **72**, 9010–9017; (*e*) N. Berova, L. Di Bari and G. Pescitelli, *Chem. Soc. Rev.*, 2007, **36**, 914–931; (*f*) G. Bringmann, T. Bruhn, K. Maksimenka and Y. Hemberger, *Eur. J. Org. Chem.*, 2009 (17), 2717–2727.

18 I. Ohtani, T. Kusumi, Y. Kashman and H. Kakisawa, *J. Am. Chem. Soc.*, 1991, **113**, 4092–4096.

19 Crystallographic data for compound **1** have been deposited with the Cambridge Crystallographic Data Centre (deposition number CCDC 859983).

20 G. M. Sheldrick, *SHELXL-97, Program for X-ray Crystal Structure Solution and Refinement*, University of Göttingen, Göttingen, Germany, 1997.

21 G. M. Sheldrick, *SADABS, Program for Empirical Absorption Correction of Area Detector Data*, University of Göttingen, Göttingen, Germany, 1999.

22 M. J. Frisch, G. W. Trucks, H. B. Schlegel, G. E. Scuseria, M. A. Robb, J. R. Cheeseman, Jr., J. A. Montgomery, T. Vreven, K. N. Kudin, J. C. Burant, J. M. Millam, S. S. Iyengar, J. Tomasi, V. Barone, B. Mennucci, M. Cossi, G. Scalmani, N. Rega, G. A. Petersson, H. Nakatsuji, M. Hada, M. Ehara, K. Toyota, R. Fukuda, J. Hasegawa, M. Ishida, T. Nakajima, Y. Honda, O. Kitao, H. Nakai, M. Klene, X. Li, J. E. Knox, H. P. Hratchian, J. B. Cross, V. Bakken, C. Adamo, J. Jaramillo, R. Gomperts, R. E. Stratmann, O. Yazyev, A. J. Austin, R. Cammi, C. Pomelli, J. W. Ochterski, P. Y. Ayala, K. Morokuma, G. A. Voth, P. Salvador, J. J. Dannenberg, V. G. Zakrzewski, S. Dapprich, A. D. Daniels, M. C. Strain, O. Farkas, D. K. Malick, A. D. Rabuck, K. Raghavachari, J. B. Foresman, J. V. Ortiz, Q. Cui, A. G. Baboul, S. Clifford, J. Cioslowski, B. B. Stefanov, G. Liu, A. Liashenko, P. Piskorz, I. Komaromi, R. L. Martin, D. J. Fox, T. Keith, M. A. Al-Laham, C. Y. Peng, A. Nanayakkara, M. Challacombe, P. M. W. Gill, B. Johnson, W. Chen, M. W. Wong, C. Gonzalez and J. A. Pople, *Gaussian 03, Revision E. 01*, Gaussian, Inc., Wallingford CT, 2004.

23 (*a*) Y. Li, S. Niu, B. Sun, S. Liu, X. Liu and Y. Che, *Org. Lett.*, 2010, **12**, 3144–3147; (*b*) Y. Wang, S. Niu, S. Liu, L. Guo and Y. Che, *Org. Lett.*, 2010, **12**, 5081–5083.

24 NCCLS documentM27-A2, NCCLS, Wayne, PA, 2002.

25 S. Khera, G. M. Woldemichael, M. P. Singh, E. Suarez and B. N. Timmermann, *J. Nat. Prod.*, 2003, **66**, 1628–1631.

